Chemical and Process Engineering: New Frontiers, 2023, 44(4), e45
DOI: 10.24425/cpe.2023.147404

A simplified method for determination of the optimal feed temperature for hydrogen peroxide decomposition in an immobilized enzyme packed-bed reactor

Ireneusz Grubecki[1*], Wirginia Tomczak[2]

[1] Cracow University of Technology, Faculty of Chemical Engineering and Technology, Warszawska 24, 31-155 Cracow, Poland
[2] Bydgoszcz University of Science and Technology, Seminaryjna 3, 85-326 Bydgoszcz, Poland

*** Corresponding author:**
e-mail:
Ireneusz.Grubecki@pk.edu.pl

Presented at 24th Polish Conference of Chemical and Process Engineering, 13–16 June 2023, Szczecin, Poland.

Article info:
Received: 31 May 2023
Revised: 27 July 2023
Accepted: 04 September 2023

Abstract
Simplified optimization method using the MATLAB function *fminbnd* was adopted to determine the optimal feed temperature (OFT) for an isothermal packed-bed reactor (PBR) performing hydrogen peroxide decomposition (HPD) with immobilized *Terminox Ultra* catalase (TUC). The feed temperature was determined to maximize (minimize) the average reactant conversion (reactant concentration) over a fixed period of time at the reactor outlet. The optimization was based on material balance and rate equation for enzyme action and decay and considered the effect of mass-transfer limitations on the system behavior. In order to highlight the relevance and applicability of the work reported here, the case of optimality under isothermal operating conditions is considered and the practical example is worked out. Optimisation method under consideration shows that inappropriate selection of the feed temperature may lead to a decrease of bioreactor productivity.

Keywords
packed-bed reactor; optimisation of bioreactors; enzyme deactivation; global mass-transfer resistances; *fminbnd* MATLAB function

1. INTRODUCTION

Dynamic bioprocess models provide valuable insight into the biotechnological industry in view of their analysis, control and optimisation. Although in this industry various types of bioreactors can be applied (De Prá et al., 2021; Li and Christofides, 2008; Lima et al., 2021), biocatalytic packed-bed bioreactors (PBR) are the most widely used (Carrié et al., 2022; Mazziero et al., 2022). This is clearly related to the fact that they offer several unique advantages, such as: increased stability of enzymes and possibility of their reuse, ease of operation and product separation as well as high process control (Carrazco-Escalante et al., 2019; Maria and Crisan, 2015; Ordaz et al., 2019; Robles et al., 2018; Schorsch et al., 2019). However, to be complete, it should be pointed out that the state variables (substrate and enzyme concentrations) as well as the temperature considered as decisive variable in tubular reactors vary both with time and space. It is worth mentioning that the effects of temperature run in opposite directions, namely, activity tends to increase with temperature as a consequence of the increase of reaction rate, while stability tends to decrease, since temperature increases the rate of enzyme inactivation. There is thus a clear compromise between enzyme activity and stability. Hence, temperature control in bioreactors has been an interesting problem from both implementation and controller design viewpoints. This is particularly true if complex microbial interactions cause significant nonlinear behaviour or/and when the model of a reactor may take the form of a set of partial differential equations referred to distributed parameter systems.

It is essential to mention that in the case of bioprocesses, biocatalyst deactivation should be additionally taken into account. As a consequence, incorporation of the extra equation describing such phenomena in the bioreactor model results in a time-varying multi-dimensional system. Hence, it is noteworthy that design and optimization of PBR are very challenging tasks. As a matter of fact, it has a significant impact on the profitability of biotechnological plant (Leipold et al., 2023).

Realistic numerical optimisation analysis with feed temperature as the decisive variable and concerning the HPD process occurring in the non-isothermal PBR in the presence of immobilized TUC (E.C. 1.11.1.6; 50,000 U/g) was previously performed (Grubecki, 2018a). A catalase with the commercial name of TUC is produced from the fungus *Scytalidium thermophilum* and constitutes a concentrated product in the form of a brown liquid meant to be diluted (Miłek, 2018). This kind of catalase is mainly used in the textile industry after textile blenching to decompose the residuals of hydrogen peroxide to water and molecular oxygen. The application of catalase enables to reduce the chemical costs by 83%, water consumption by 50%, energy consumption by 48% and processing time by 33% (Eberhardt et al., 2004).

However, in the case of HPD, the mathematical model can be significantly simplified as in the industrial practise it runs at the hydrogen peroxide (HP) concentrations lower than 2×10^{-2} kmol·m^{-3} (Miłek, 2020). In consequence, the heat released during the reaction makes the temperature conditions to be isothermal ones (Xiu et al., 2001).

© 2023. The Author(s). This is an open-access article distributed under the terms of the Creative Commons Attribution (CC-BY 4.0, https://creativecommons.org/licenses/by/4.0/), which permits unrestricted use, distribution, and reproduction in any medium, provided the original author and source are credited.

Moreover, geometry of the model reactor makes the axial dispersion in the bulk liquid phase minimized.

From the viewpoint of design calculations such assumptions are essential since the mathematical model describing the HPD consists only of the equations of unsteady-state continuous mass balance and rate of enzyme inactivation. In such a case, it is possible to find analytical expressions for HP and active TUC concentrations. Such an analytical solution makes the finding of the optimal solution for the issue presented in the previous work (Grubecki, 2018a) simpler.

Given the background described above, the goal of this paper was to perform the optimisation procedure to search for the feed temperature in the bioreactor for HPD packed with immobilized TUC undergoing parallel deactivation (dependent on HP concentration) using the simplified method. The feed temperature was evaluated to maximize the time-average substrate conversion over a given period at the fixed feed flow rate, accounting for the lower $T_{\min} = 293$ K and upper $T_{\max} = 323$ K permissible temperatures as well as diffusional restrictions expressed by the global effectiveness factor.

The approach presented in this paper makes it possible to define the operational conditions at which efficiency of the PBR used for the decomposition process of HP by immobilized TUC reaches a maximum or is the highest.

2. MATHEMATICAL APPROACH

2.1. Quantitative description of the fixed-bed bioreactor

In the HPD process the rate of changes in the substrate concentration $(-r_S)$ – after taking into consideration the mass-transfer resistances – can be described by the Michaelis–Menten kinetics (Fruhwirth et al., 2002; Grubecki, 2010a; 2010b):

$$(-r_S) = \eta_{\text{eff}} k_R \frac{C_E C_S}{(1 + C_S/K_M)} \tag{1}$$

In industrial practice HPD runs at low HP concentration (lower than or equal to 0.02 kmol·m^{-3}), therefore, it can be assumed that $C_S \ll K_M$. Then, Equation (1) can be simplified and expressed as follows (Arvin and Lars-Flemming, 2015; Ghadermarzi and Moosavi-Movahedi, 1996; Trawczyńska, 2020):

$$(-r_S) = \eta_{\text{eff}} k_R C_E C_S \tag{2}$$

Low concentration makes the process under consideration isothermal and pseudo-homogeneous. Bearing this in mind, for decomposition process of HP taking place under industrial conditions in a tubular (column) reactor packed with immobilized enzyme – after taking into account the diffusional resistances – the unsteady material balance on substrate is:

$$\begin{aligned} [\varepsilon_f + (1-\varepsilon_f)\varepsilon_p] \frac{\partial C_S}{\partial t} + U_f \varepsilon_f \frac{\partial C_S}{\partial x} = \\ - \eta_{\text{eff}} (1-\varepsilon_f)(1-\varepsilon_p) k_R C_E C_S, \\ C_S(x=0,t) = C_{S,\text{In}} \end{aligned} \tag{3}$$

Each enzymatic reaction is accompanied by decreased catalytic potential of an enzyme (Baral et al., 2023; Goldsmith and Tawfik, 2017; Illanes et al., 2014; Liu et al., 2022; Mehrotra et al., 2020; Razavi et al., 2016; Samson et al., 2018; Sooch et al., 2014; Vishnu Priya et al., 2022). In line with the results of George (1947) theoretically verified by Vasudevan and Weiland (1990), the expression describing changes in the rate of biocatalyst inactivation caused by reactant (hydrogen peroxide) inhibition must also have a Michaelis–Menten form. At a low reactant concentration, accounting for the diffusional resistances, inactivation rate equation can be approximated by:

$$-\frac{\mathrm{d}C_E}{\mathrm{d}t} = \eta_{\text{eff}} (1-\varepsilon_f) k_D C_E C_S, \quad C_E(x, t=0) = C_{E0} \tag{4}$$

Worthy of note, such form of Eq. (4) can usually be employed in the studies of immobilized catalase in a PBR regardless of which method of immobilization is used (Danial and Alkhalaf, 2020; Do and Weiland, 1981a; 1981b; Grigoras, 2017; Sun et al., 2019).

The impact of temperature on the reaction ν_R ($k_R = \nu_R/K_M$) and deactivation ν_D ($k_D = \nu_D/K_D$) rate constants are described by the Arrhenius equation:

$$k_R^* = k_{R0} \exp\left(-\frac{E_R}{RT}\right), \quad k_D = k_{D0} \exp\left(-\frac{E_D}{RT}\right) \tag{5}$$

By rescaling according to:

$$E = \frac{C_E}{C_{E0}} = \frac{C_S}{C_{S,\text{In}}} \tag{6}$$

$$X = \frac{x}{H}, \quad \tau = t \frac{U_f \varepsilon_f}{[\varepsilon_f + (1-\varepsilon_f)\varepsilon_p] H} \tag{7}$$

$$\begin{aligned} \chi_R &= k_R a_m \frac{(1-\varepsilon_f)(1-\varepsilon_p)}{(U_f \varepsilon_f)} H \\ \chi_D &= \frac{k_D C_{S,\text{In}}}{k_R a_m} \cdot \frac{[\varepsilon_f + (1-\varepsilon_f)\varepsilon_p]}{(1-\varepsilon_p)} \end{aligned} \tag{8}$$

the partial differential equations for mass balance in the bulk liquid as well as for the biocatalyst deactivation rate which constitute the quantitative description of the HPD course in a PBR can be put into the following dimensionless form:

$$\frac{\partial S}{\partial \tau} + \frac{\partial S}{\partial X} = -\eta_{\text{eff}} \chi_R E S, \quad S(0,\tau) = 1, \tag{9a}$$

$$\frac{\partial E}{\partial \tau} = -\eta_{\text{eff}} \chi_R \chi_D E S, \quad E(X,0) = 1 \tag{9b}$$

2.2. Mass-transfer resistance evaluation

When the enzyme is contained within a solid matrix, mass transfer limitations may severely restrain the expression of the catalytic potential. Then, it is necessary to assess the effect of diffusional restrictions to properly evaluate the biocatalyst performance. Considering the enzyme immobilization on porous carriers, internal mass transfer (pore diffusion) is usually dominant compared to external mass transfer (film diffusion). However, in the case of the HPD process occurring in the presence of immobilized TUC the external diffusional resistances (EDR) (Grubecki, 2017) and global diffusional resistances are to be considered. The magnitude of the diffusional resistances can be conveniently expressed by means of the biocatalyst effectiveness factor, which constitutes a general concept that represents the ratio of rates of a phenomenon under the influence of a diffusional resistances and freed from that influence. For the HPD process, the effectiveness transfer that characterizes the global diffusional limitations ($\eta_{\text{eff}} = \eta_G$) takes the form (Appendix A):

$$\eta_G = \frac{1}{3\Phi^2} \cdot \frac{(3\Phi) \cdot \coth(3\Phi) - 1}{\left(1 - \frac{1}{\text{Bi}_M}\right) + \left(\frac{3\Phi}{\text{Bi}_M}\right) \cdot \coth(3\Phi)} \tag{10}$$

where Biot number, Bi_M, and Thiele modulus, Φ, are given by:

$$\text{Bi}_M = \frac{d_P k_L}{6 D_{\text{eff}}} \tag{11}$$

$$\Phi = \frac{d_P}{6} \sqrt{\frac{k_R a_m}{D_{\text{eff}}}} \tag{12}$$

The mathematical model expressed by Eqs. (9a) and (9b) including the expressions (10)–(12) revealing the influence of mass-transfer limitation allows to foresee the behaviour of the reactor packed with immobilized TUC decomposing the HP residuals under industrial applications.

3. OPTIMIZATION, PROBLEM STATEMENT

The analysis deals with the packed-bed bioreactor described in detail in the previously published paper (Grubecki, 2018a). To make this considerations clearer, the flow sheet of the tubular bioreactor packed with immobilized enzyme used in the experiment has been illustrated again in Figure 1. TUC was immobilized by glutaraldehyde-coupling to the silanised support according to the method of Malikkides and Weiland (1982). A more detailed description of the experimental procedure has been provided in the paper published previously (Grubecki, 2017).

In the ideal tubular bioreactor presented in Fig. 1 the convection phenomena dominate over dispersive ones. In such reactors, alongside the feed flow rate, temperature is the most important control variable that affects the rates of both enzymatic reaction and enzyme inactivation depending on the value of operating temperature, as well as the mutual relation between the activation energies for reaction and deactivation. Therefore, such temperature strategy can be established that guarantees an inherent trade-off between various and conflicting objectives, and – as a result – the maximum (bio)reactor productivity (Agrawal and Verma, 2019; Coutu et al., 2023; Grubecki, 2016; Grubecki and Wójcik, 2013; Harmand and Dochain, 2005; Harmand et al., 2008; Maria and Crisan, 2015; Ortega et al., 2021; Tezer et al., 2023).

Finding such a temperature strategy is a challenging and delicate task and more advanced optimisation procedures are needed due to complicated dynamics of biotransformations. However, in the case of enzymatic decomposition of HP the optimisation procedure can be significantly simplified due to irrelevant thermal effect caused by the low HP concentration (Miłek, 2018; Miłek, 2020), by which HPD process can be considered as isothermal one.

Thus, the key issue is to find the feed temperature that under operating conditions would provide the maximum time-average productivity at the reactor outlet.

The problem under consideration was already discussed previously (Grubecki, 2018a; 2018b). However, in industrial practice the quick assessment of optimal operating conditions is usually required. Hence, the most comfortable situation is when the problem under consideration can be described with an analytical equation. This situation is also encountered in the HPD process since the solution of the mathematical model (Eqs. (9) and (10)) can be derived analytically.

3.1. Analytical description of the HPD process behavior

Considering the isothermal process of HPD, it is possible to derive mathematical expressions for hydrogen peroxide and active enzyme concentrations as functions of dimensionless distance from the reactor inlet (X) and nondimensional time (τ) (Appendix B):

$$S(X,\tau) = \frac{\exp[\eta_{\text{eff}} \chi_R \chi_D \cdot (\tau - X)]}{\exp(\eta_{\text{eff}} \chi_R \cdot X) + \exp[\eta_{\text{eff}} \chi_R \chi_D \cdot (\tau - X)] - 1} \tag{13a}$$

$$E(X,\tau) = \frac{\exp[\eta_{\text{eff}} \chi_R \cdot X]}{\exp(\eta_{\text{eff}} \chi_R \cdot X) + \exp[\eta_{\text{eff}} \chi_R \chi_D \cdot (\tau - X)] - 1} \tag{13b}$$

Equations (13a) and (13b) describe the behavior of the immobilized enzyme packed-bed bioreactor used for decomposition of hydrogen peroxide.

3.2. Objective function

The goal of optimization was to find the feed temperature that under a constant feed flow rate maximizes (minimizes) time-averaged HP conversion, α_m (HP concentration, S_m),

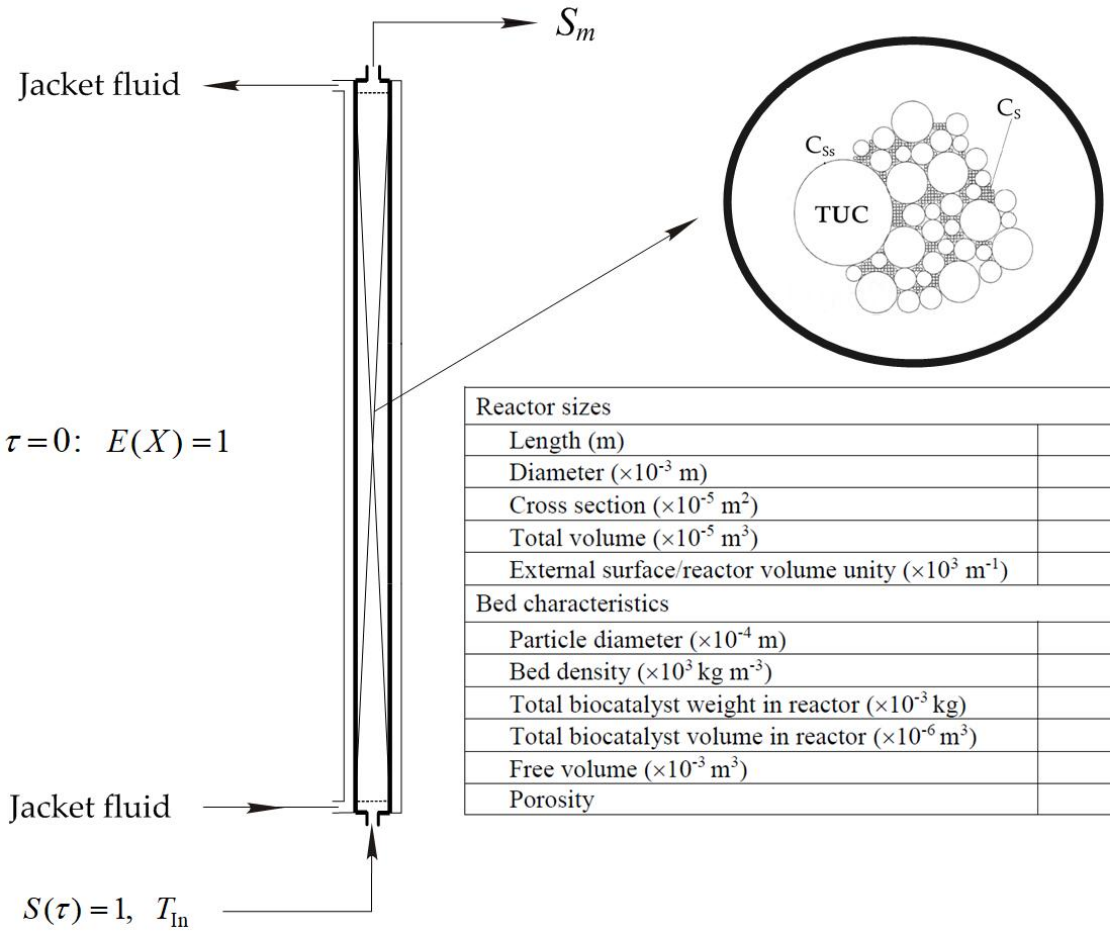

Reactor sizes	
Length (m)	0.36
Diameter ($\times 10^{-3}$ m)	8.00
Cross section ($\times 10^{-5}$ m^2)	5.03
Total volume ($\times 10^{-5}$ m^3)	1.81
External surface/reactor volume unity ($\times 10^3$ m^{-1})	8.32
Bed characteristics	
Particle diameter ($\times 10^{-4}$ m)	5.05
Bed density ($\times 10^3$ kg m^{-3})	1.82
Total biocatalyst weight in reactor ($\times 10^{-3}$ kg)	33.0
Total biocatalyst volume in reactor ($\times 10^{-6}$ m^3)	12.67
Free volume ($\times 10^{-3}$ m^3)	5.43
Porosity	0.30

Figure 1. Flow sheet of PBR for decomposition process of HP.

at the bioreactor outlet. Thus, the objective function can be defined in the form of Eq. (14):

$$\alpha_m(T) = \frac{1}{\tau_f}\int_0^{\tau_f}[1 - S(X = 1, \upsilon, T)]\mathrm{d}\upsilon = 1 - \frac{1}{\tau_f}\int_0^{\tau_f} S(X = 1, \upsilon, T)\mathrm{d}\upsilon = 1 - S_m(T) \quad (14)$$

As the optimization problems expressed by Eq. (14) are mathematically equivalent, let us minimize the time-averaged HP concentration. Then, the objective function adopted for the further analysis takes the following form:

$$S_m(T) = \frac{1}{\tau_f}\int_0^{\tau_f}\frac{\exp[\eta_{\mathrm{eff}}(T)\chi_R(T)\chi_D(T)\cdot(\upsilon-1)]}{\exp[\eta_{\mathrm{eff}}(T)\chi_R(T)]+\exp[\eta_{\mathrm{eff}}(T)\chi_R(T)\chi_D(T)\cdot(\upsilon-1)]-1}\mathrm{d}\upsilon \quad (15)$$

Integrating Equation (15) according to the integration limits, we get the function of the temperature, T, considered to be the control variable, as follows:

$$S_m(T) = \frac{1}{\eta_{\mathrm{eff}}(T)\,\chi_R(T)\chi_D(T)\tau_f}\times \ln\left\{\frac{\exp[\eta_{\mathrm{eff}}(T)\chi_R(T)]+\exp[\eta_{\mathrm{eff}}(T)\chi_R(T)\chi_D(T)\cdot(\tau_f-1)]-1}{\exp[\eta_{\mathrm{eff}}(T)\chi_R(T)]+\exp[-\eta_{\mathrm{eff}}(T)\chi_R(T)\chi_D(T)]-1}\right\} \quad (16)$$

3.3. Simplified numerical optimization

The presented optimization problem is not a complicated issue and can be solved numerically or analytically using the method of differential calculus of the single-variable function.

However, more convenient method of numerical optimization is the application of *fminbnd* function of MATLAB® Optimization Toolbox (MATLAB, 2019). This function can be used to find the minimum of a single-variable function on a fixed interval.

To use the *fminbnd* function the following syntax command line is required:

$$[a, f\mathrm{value}] = \mathit{fminbnd}(@\mathrm{objectfun}, a_1, a_2, \mathit{options}) \quad (17)$$

The function of *fminbnd* returns a value a that is a local minimizer of the scalar valued function that is described in

@objectfun in the interval $a_1 < a < a_2$, *options* enables to create or modify the structure of the optimization options.

In the case under consideration, the optimization problem can be described by the performance index with a constraint as given bellow:

Minimize

$$S_m(T) = \frac{1}{\eta_{\text{eff}}(T)\,\chi_R(T)\chi_D(T)\tau_f} \times \times \ln\left\{\frac{\exp[\eta_{\text{eff}}(T)\cdot\chi_R(T)]+\exp[\eta_{\text{eff}}(T)\cdot\chi_R(T)\chi_D(T)\cdot(\tau_f-1)]-1}{\exp[\eta_{\text{eff}}(T)\cdot\chi_R(T)]+\exp[-\eta_{\text{eff}}(T)\cdot\chi_R(T)\chi_D(T)]-1}\right\} \quad (18)$$

Subject to

$$\chi_R(T) = k_R(T)a_m(1-\varepsilon_f)(1-\varepsilon_p)\frac{V_R}{Q} \quad (19)$$

$$\chi_D(T) = \frac{k_D(T)C_{S,\text{In}}}{k_R(T)a_m}\cdot[\varepsilon_f + (1-\varepsilon_f)\varepsilon_p] \quad (20)$$

$$k_R(T)a_m = k_{R0}a_m \exp\left(-\frac{E_R}{RT}\right)$$
$$k_D(T) = k_{D0}\exp\left(-\frac{E_D}{RT}\right) \quad (21)$$

$$\eta_{\text{eff}}[\text{Bi}_M(T), \Phi(T)] = \frac{1}{3\Phi^2}\cdot\frac{(3\Phi)\cdot\coth(3\Phi)-1}{\left(1-\frac{1}{\text{Bi}_M}\right)+\left(\frac{3\Phi}{\text{Bi}_M}\right)\cdot\coth(3\Phi)} \quad (22)$$

$$\text{Bi}_M(T) = \frac{d_P k_L(T)}{6D_{\text{eff}}} \quad (23)$$

$$k_L(T) = 1.132\frac{D_{L,S}^{0.667}}{D_R^{0.632}d_p^{0.368}}\left[\frac{\rho(T)}{\eta(T)}\right]^{0.3}Q^{0.632} \quad (24)$$

$$\Phi(T) = \frac{d_P}{6}\sqrt{\frac{k_R(T)a_m}{D_{\text{eff}}}} \quad (25)$$

Constraint

$$T_{\min} \le T \le T_{\max} \quad (26)$$

The method described above is a convenient and quick optimization tool and can be used for any problem minimizing (maximizing) the one-variable function with the upper and lower constraints on the control variable.

4. RESULTS AND DISCUSSION

The enzymatic reactor under consideration was optimized using Eqs. (9)–(12) as well as (18)–(26) with the kinetic constants reported in Table 1 (Grubecki, 2017).

For TUC, due to its optimal operational activity, the temperature range with permissible lower $T_{\min} = 293$ K and upper $T_{\max} = 323$ K limits has been taken into consideration.

A great convenience of the simplified optimisation method has been presented in Figures (2)–(4) showing the effect of feed flow rate (Fig. 2), feed substrate concentration (Fig. 3) and total time (Fig. 4) on the time-average HP conversion in the outstream, α_m, as well as activity of biocatalyst, E_m, undergoing parallel deactivation, as a function of the feed temperature.

Table 1. Kinetics parameters used in the optimization study.

Reaction of hydrogen peroxide decomposition	
Activation energy [kJ mol^{-1}]	$E_R = 12.6 \pm 0.3$
Frequency factor [s^{-1}]	$k_{R0}a_m = 48.00 \pm 5.38$
Deactivation of Terminox Ultra catalase	
Activation energy [kJ mol^{-1}]	$E_D = 49.7 \pm 1.2$
Frequency factor [m^3 kmol^{-1} s^{-1}]	$k_{D0} = (2.77 \pm 1.08) \times 10^7$

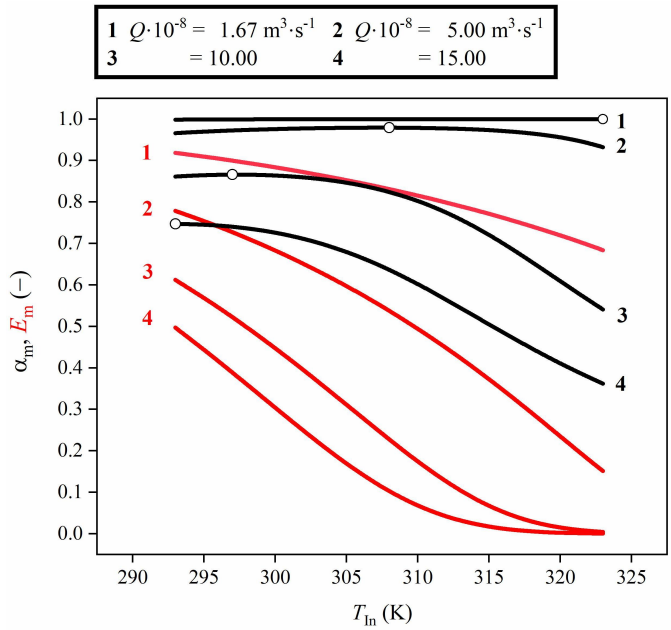

Figure 2. Time-average HP conversion, α_m (black lines), and TUC activity, E_m (red lines) as functions of feed temperature, T_{In}, and feed flow rate, Q, for $C_{S,\text{In}} = 5 \cdot 10^{-3}$ kmol·m^{-3} and $\tau_f = 16$ h. Open symbols represent the maximum values of time-average conversion.

In the process of HPD proceeding in the presence of TUC undergoing deactivation dependent on HP concentration there exists the feed temperature that makes the time-average HP conversion maximal or the highest. Results of analysis have shown that the higher the difference between the upper and the lower allowable temperatures, the more OFT is likely to occur.

In order to prove the validity of the last statement it is worth quoting the sufficient condition for local extremum of any single-variable function f.

Theorem 1: *Let $c \in [a, b]$ and f be continuous at c. If for some $\delta > 0$, f is increasing (decreasing) on $(c - \delta, c)$ and decreasing (increasing) on $(c, c + \delta)$, then f has a local maximum (minimum) at c.*

Based on this theorem such feed temperature $T_{\mathrm{In}}^{\bullet}$ can be indicated that for feed temperature T_{In} in left-hand side neighborhood of $T_{\mathrm{In}}^{\bullet}$ ($T_{\mathrm{In}} < T_{\mathrm{In}}^{\bullet}$) time-average reactant conversion, and at the same time productivity, increases when temperature T_{In} grows. In turn, for the feed temperature T_{In} in the right-hand side neighborhood of $T_{\mathrm{In}}^{\bullet}$ ($T_{\mathrm{In}} > T_{\mathrm{In}}^{\bullet}$), time-average conversion decreases when feed temperature raises. This means that such feed temperature can be indicated for which the time-average HP conversion reaches the maximum. When the temperature maximizing the time-average reactant conversion is lower than T_{min} or higher than T_{max}, then OFT takes values of T_{min} and T_{max}, respectively.

Based on results presented in Figures 2–4 it can be indicated that the selection of unsuitable temperature, especially in the case of higher values of feed flow rates, feed concentrations and biocatalyst ages, makes the HPD process with parallel TUC deactivation to be less efficient.

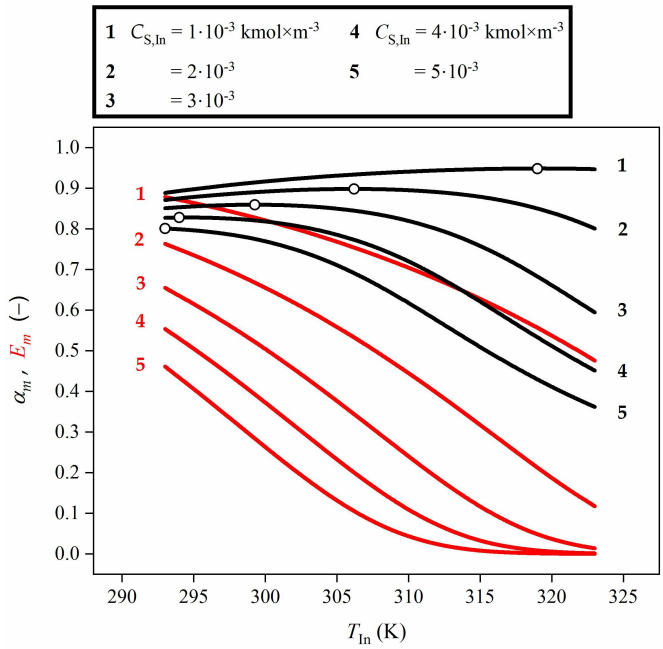

Figure 3. Time-average HP conversion, α_m (black lines), and TUC activity, E_m (red lines) as functions of feed temperature, T_{In}, and feed HP concentration, $C_{S,\mathrm{In}}$, for $\tau_f = 16$ h and $Q = 25 \cdot 10^{-8}$ m^3·s^{-1}.

Figure 4 shows the significant effect of the feed temperature – and at the same time temperature within the PBR – and total time on time-average substrate conversion. If we want to extend the biocatalyst age from 8h to 16h, the OFT should decrease from 323 K to 307.6 K. Further age increase up to 24 h, 32 h, and finally up to 40h requires reducing the OFT to 303 K, 296 K, and 293 K, respectively.

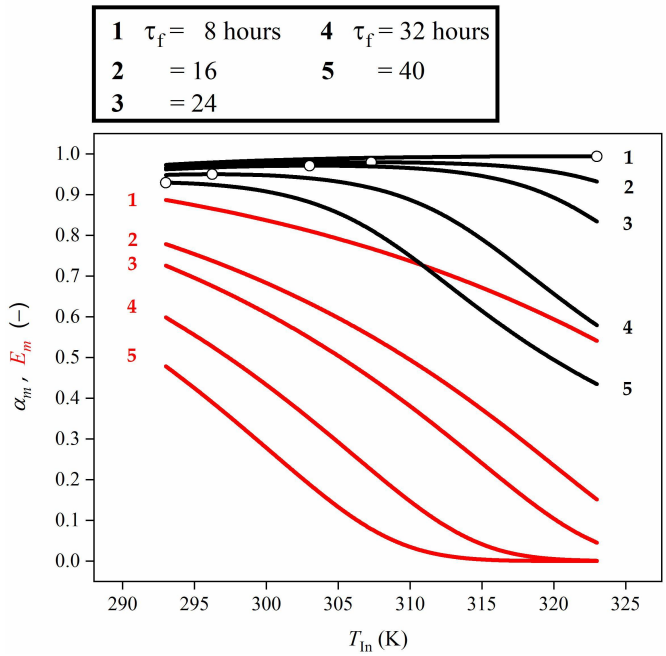

Figure 4. Time-average HP conversion, α_m (black lines), and TUC activity, E_m (red lines) as functions of feed temperature, T_{In}, and total time, τ_f, for $C_{S,\mathrm{In}} = 5 \cdot 10^{-3}$ kmol·m^{-3} and $Q = 5 \cdot 10^{-8}$ m^3·s^{-1}.

The above-mentioned regularities indicate the general rules for determining the optimal feed control for enzymatic reaction, especially HPD, catalysed by immobilized enzyme, especially TUC, undergoing inactivation. The feed flow rate considered as a control variable should be defined as a diminishing function of time to extend the contact time between a biocatalyst with decreasing activity and the reaction mixture flowing through the reactor.

The reasoning is simple since the lower feed flow rate leads to the lower substrate concentration at the biocatalyst surface. In consequence, the slower biocatalyst deactivation can be expected yielding the higher HP consumption at the reactor outlet.

In order to verify the model-based predictions of the feed temperature ensuring the maximum efficiency of the tubular reactor packed with immobilized catalase, a comparison of the observed time-averaged HP conversions obtained for OFT with those predicted theoretically using simplified optimization method is shown in Figure 5.

The presented results indicated that in the HPD process occurring under EDR the time-averaged HP conversions obtained theoretically using Eq. (18) for OFT calculated by means of *fminbnd* function is convergent to those observed at the outlet of the model plug-flow reactor (Fig. 1) operated under OFT with the normalized deviation lower than 4.0%.

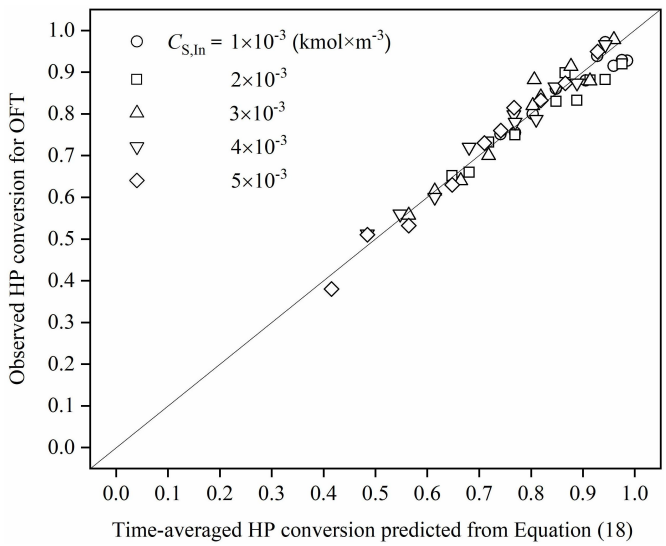

Figure 5. The comparison between observed time-averaged HP conversions obtained for OFT and those calculated from Eq. (18) for $Q \cdot 10^8 = 10$ and 12 m^3·s^{-1} and total time τ_f considered in Fig. 4.

5. CONCLUSIONS

In the current study, a simplified optimization method using the MATLAB function *fminbnd* has been applied to assess the feed temperature ensuring the maximum efficiency of the ideal tubular reactor packed with immobilized enzyme and operating under unsteady state conditions.

The reasoning which is based on an analytical solution is relevant for the predesign steps because it indicates in a simple fashion which inlet temperature should be followed in order to obtain the maximum advantage of existing enzyme using the type of reactor usually elected by technologists in fine bioprocess engineering field.

The analysis contributes to better understanding of the engineering aspects of immobilized enzyme reactor design accounting for mass-transfer phenomena. It should be clearly emphasized that temperature exerts a crucial impact and poses a compromise between the biocatalyst activity and stability. Hence, adjusting the appropriate temperature policy yielding the required substrate consumption at the reactor outlet is the essential part to ensure the desired operating conditions accompanying biotransformation running in packed-bed bioreactor. To obtain constant substrate conversion at the reactor outstream, decreasing flowrate to follow enzyme deactivation rate is recommended.

The methodology presented in this paper may prove especially useful for the design and evaluation of reactor performance with immobilized enzymes subjected to diffusional restrictions and activity loss during operation.

SYMBOLS

a_m	specific surface area, m^2/m^3
Bi_M	Biot number ($= k_L d_P / 6 D_{\mathrm{eff}}$)
C_S	bulk substrate concentration, kmol/m^3
$C_{S,\mathrm{In}}$	H_2O_2 concentration at the inlet ($j = \mathrm{In}$), kmol/m^3
C_E	enzyme activity, kg/m^3
d_P	diameter of the pellet, m
$D_{L,S}$	diffusion coefficient of the substrate, m^2/s
D_{eff}	effective diffusivity of the substrate in catalyst particle, m^2/s
E	nondimensional biocatalyst activity
E_i	activation energy for reaction ($i = \mathrm{R}$) and deactivation ($i = \mathrm{D}$), J/mol
H	reactor length, m
K_i	Michaelis constant for reaction ($i = \mathrm{M}$) and deactivation ($i = \mathrm{D}$), kmol/m^3
k_L	volumetric mass transfer coefficient, m/s
k_D	modified deactivation rate constant ($= \nu_{\mathrm{D}}/K_{\mathrm{D}}$), m^3/(kmol·s)
k_{D0}	frequency factor for deactivation rate constant, m^3/(kmol·s)
k'_{R}	modified reaction rate constant ($= \nu_{\mathrm{R}}/K_{\mathrm{M}}$), m^3/(kg·s)
k_{R0}	frequency factor for enzymatic reaction rate constant, m/s
k_{R}	reaction rate constant ($= k'_{\mathrm{R}} C_{E0}/a_{\mathrm{m}}$), m/s
Q	feed flow rate, m^3/s
S	nondimensional substrate concentration
t	time, s
T_{In}	inlet temperature, K
x	axial position in the reactor, m
X	nondimensional axial position in the reactor ($= x/H$)

Greek symbols

$\varepsilon_f, \varepsilon_p$	porosity of the bulk fluid ($= 0.3$) and particulate phases, respectively
Φ	Thiele modulus ($= d_{\mathrm{p}}/6 \cdot (k_{\mathrm{R}} a_{\mathrm{m}}/D_{\mathrm{eff}})^{1/2}$)
$\chi_{\mathrm{R}}, \chi_{\mathrm{D}}$	dimensionless numbers defined by Eq. (7)
ν	dynamic viscosity of the bulk fluid phase, kg/(m·s)
η_{eff}	biocatalyst effectiveness factor defined by Eq. (10)
ν_{D}	deactivation rate constant, 1/s
ν_{R}	reaction rate constant, kmol/(kg·s)
ρ	density of the bulk fluid phase, kg/m^3
τ	nondimensional time defined by Eq. (5)

A. APPENDIX

Effectiveness factor of global mass transfer phenomenon

The material balance considering kinetics of first-order enzymatic reaction and mass-transfer rate can be expressed in the following dimensionless form:

$$\frac{\mathrm{d}^2 S_{\mathrm{Int}}}{\mathrm{d}\xi^2} + \frac{2}{\xi}\frac{\mathrm{d}S_{\mathrm{Int}}}{\mathrm{d}\xi} - 9\Phi^2 S_{\mathrm{Int}} = 0 \qquad \text{(A.1)}$$

where $\xi = r/R$, $S_{\text{Int}} = C_{S,\text{Int}}/C_{S0}$, and Φ is Thiele modulus, and C_{S0} is substrate concentration in the biofilm.

In the case of significant external diffusional resistance, substrate concentration at the liquid–particle interface will differ from that in the bulk. Then, the combined effect of EDR and IDR should be taken into account by introduction of boundary conditions described the symmetry of distribution (Eq. (A.2a)) and continuity at the liquid–catalyst interface (Eq. (A.2b)):

$$\frac{dS_{\text{Int}}}{d\xi} = 0 \quad \text{at} \quad \xi = 0 \tag{A.2a}$$

$$\text{Bi}_M[S_0 - S_S] = \left.\frac{dS_{\text{Int}}}{d\xi}\right|_{\xi=1} \tag{A.2b}$$

where Bi_M is the Biot number ($= k_L \cdot d_P/(6D_{L,S})$), S_0 and S_S are the dimensionless substrate concentration in biofilm and substrate concentration at the surface of biocatalyst, respectively.

Introducing the new variable: $y = S_{\text{Int}}(\xi) \cdot \xi$ into Eq. (A.1) the profile of substrate concentration can be found in the following form:

$$S_{\text{Int}}(\xi) = A_1 \frac{\sinh(3\Phi \cdot \xi)}{\xi} + A_2 \frac{\cosh(3\Phi \cdot \xi)}{\xi} \tag{A.3}$$

where A_1, A_2 are the integration constants.

It is known that when $r \to 0$ then $\sinh(3\Phi \cdot \xi)/\xi \to 3\Phi$ and $\cosh(3\Phi \cdot \xi)/\xi \to \infty$. Thus, to obtain the constant substrate concentration inside the biocatalyst pellet integration coefficient A_2 have to vanish ($A_2 = 0$). Hence, the expression for substrate concentration and its first derivative take the forms:

$$S_{\text{Int}}(\xi) = A_1 \frac{\sinh(3\Phi \cdot \xi)}{\xi} \tag{A.4}$$

$$\frac{\text{d}S_{\text{Int}}}{\text{d}\xi} = A_1 \frac{3\Phi\xi \cdot \cosh(3\Phi \cdot \xi) - \sinh(3\Phi \cdot \xi)}{\xi^2} \tag{A.5}$$

Using the boundary condition (A.2b) it is possible to evaluate the constant A_1:

$$\left(\frac{\text{d}S_{\text{Int}}}{\text{d}\xi}\right)_{\xi=1} = A_1 \cdot [3\Phi \cdot \cosh(3\Phi) - \sinh(3\Phi)] = \text{Bi}_M(S_0 - S_S) = \text{Bi}_M(S_0 - S_{\text{Int}}(\xi = 1)) = \text{Bi}_M[S_0 - A_1 \sinh(3\Phi)]$$

Hence, the following expression for A_1 is obtained:

$$A_1 = S_0 \cdot \left[\frac{3\Phi}{\text{Bi}_M}\cosh(3\Phi) + \left(1 - \frac{1}{\text{Bi}_M}\right) \cdot \sinh(3\Phi)\right]^{-1} \tag{A.6}$$

Thus, exact solution in a dimensionless form may be written as follows:

$$S_{\text{Int}}(\xi) = S_0 \cdot \left[\frac{(3\Phi)}{\text{Bi}_M}\cosh(3\Phi) + \left(1 - \frac{1}{\text{Bi}_M}\right) \cdot \sinh(3\Phi)\right]^{-1} \cdot \frac{\sinh(3\Phi \cdot \xi)}{\xi} \tag{A.7}$$

Let us define the global effectiveness factor:

$$\eta_G = \frac{\text{observed reaction rate in biocatalyst}}{\text{reaction rate in biofilm}} = \frac{A_S}{V_S} \cdot \frac{r_{S,\text{obs}}(C_{S,\text{Int}})}{r_S[C_{S0}]} \tag{A.8}$$

Then, the use of Eq. (A.6) yields

$$\eta_G = \frac{A_S}{V_S} \frac{D_{L,S}\left(\frac{\text{d}C_{S,\text{Int}}}{\text{d}r}\right)_{r=R}}{r_S[C_S(R)]} = 3\Phi^{-2} \frac{\left(\frac{\text{d}S_{\text{Int}}}{\text{d}\xi}\right)_{\xi=1}}{S_0} = 3\Phi^{-2} \cdot \frac{S_0\left[\frac{3\Phi}{\text{Bi}_M}\cosh(3\Phi) + \left(1 - \frac{1}{\text{Bi}_M}\right) \cdot \sinh(3\Phi)\right]^{-1}[3\Phi \cdot \cosh(3\Phi) - \sinh(3\Phi)]}{S_0}$$

Finally, the expression for the global effectiveness factor is as follows:

$$\eta_G = \Phi^{-1} \cdot \frac{\coth(3\Phi) - (3\Phi)^{-1}}{\left(1 - \frac{1}{\text{Bi}_M}\right) + \left(\frac{3\Phi}{\text{Bi}_M}\right) \cdot \coth(3\Phi)} \tag{A.9}$$

If EDR is insignificant ($\text{Bi} \gg 1$), Equation (A.9) can be reduced to the equation presented below and describing the internal effectiveness factor:

$$\eta_G = \eta_{\text{IDR}} = \Phi^{-1} \cdot \frac{\coth(3\Phi) - (3\Phi)^{-1}}{\left(1 - \frac{1}{\text{Bi}_M}\right) + \frac{(3\Phi)}{\text{Bi}_M} \cdot \coth(3\Phi)} = \Phi^{-1} \cdot [\coth(3\Phi) - (3\Phi)^{-1}] \tag{A.10}$$

B. APPENDIX

Analytical approach for prediction of immobilized enzyme packed-bed bioreactor behavior

For the isothermal packed-bed reactor with plug flow operating under unsteady state, the differential mass balance for HP concentration in the bulk liquid phase as well as differential equation for the TUC inactivation can be written in the following form:

$$\frac{\partial S}{\partial \tau} + \frac{\partial S}{\partial X} = -\eta_{\text{eff}}\chi_R \cdot ES, \qquad S(0,\tau) = 1 \tag{B.1a}$$

$$\frac{\partial E}{\partial \tau} = -\eta_{\text{eff}}\chi_R\chi_D ES, \qquad E(X,0) = 1 \tag{B.1b}$$

where

$$E = \frac{C_E}{C_{E0}}, \qquad S = \frac{C_S}{C_{S,\text{In}}} \tag{B.2}$$

$$X = \frac{x}{H}, \qquad \tau = t\frac{U_f\varepsilon_f}{[\varepsilon_f + (1-\varepsilon_f)\varepsilon_p]H} \tag{B.3}$$

$$\chi_R = k_R a_m \frac{(1-\varepsilon_f)(1-\varepsilon_p)}{(U_f\varepsilon_f)}H, \qquad \chi_D = \frac{k_D C_{S,\text{In}}}{k_R a_m} \cdot \frac{[\varepsilon_f + (1-\varepsilon_f)\varepsilon_p]}{(1-\varepsilon_p)} \tag{B.4}$$

To solve the equation system (B.1)–(B.4) the following transformation should be made:

$$\tau^\bullet = \tau - X, \qquad X^\bullet = X \tag{B.5}$$

Then, equation system (B.1) with boundary conditions becomes:

$$\frac{\partial S}{\partial X^\bullet} = -\eta_{\text{eff}}\chi_R ES, \qquad S(X^\bullet = 0, \tau^\bullet) = 1 \tag{B.6a}$$

$$\frac{\partial E}{\partial \tau^\bullet} = -\eta_{\text{eff}}\chi_R\chi_D ES, \qquad E(X^\bullet, \tau^\bullet = 0) = 1 \tag{B.6b}$$

Equations (B.6a) and (B.6b) describe enzyme and hydrogen peroxide behaviour in the case when the last one is influenced by inlet concentration.

Due to a similar form of the right-hand side of the state equations it is possible to divide Eqs. (B.6a) and (B.6b) side by side. Then

$$\frac{\partial S}{\partial E} = \frac{1}{\chi_D}\frac{\partial X^\bullet}{\partial \tau^\bullet} \tag{B.7}$$

Considering Eq. (B.7) it can be clearly stated that there exists a function $\Lambda(X^\bullet, \tau^\bullet)$ such that

$$\frac{\partial S}{\partial X^\bullet} = \frac{1}{\chi_D}\frac{\partial^2 \Lambda}{\partial X^\bullet \partial \tau^\bullet} \wedge \frac{\partial E}{\partial \tau^\bullet} = \frac{\partial^2 \Lambda}{\partial X^\bullet \partial \tau^\bullet}$$
$$\text{or} \quad S = \frac{1}{\chi_D}\frac{\partial \Lambda}{\partial \tau^\bullet} \wedge E = \frac{\partial \Lambda}{\partial X^\bullet} \tag{B.8}$$

satisfying Eq. (B.7).

Accounting for Eq. (B.8) in the mathematical model (B.1) and rearranging, we get:

$$\frac{\partial^2 \Lambda}{\partial X^\bullet \partial \tau^\bullet} + \eta_{\text{eff}}\chi_R \frac{\partial \Lambda}{\partial X^\bullet}\frac{\partial \Lambda}{\partial \tau^\bullet} = 0 \tag{B.9}$$

Let us predict the following form of the function fulfilling the above equation (B.9):

$$\Lambda(X^\bullet, \tau^\bullet) = (\eta_{\text{eff}}\chi_R)^{-1} \ln[\lambda(X^\bullet, \tau^\bullet)] \tag{B.10}$$

Combining Eqs. (B.9) and (B.10) yields:

$$\frac{\partial^2 \lambda}{\partial X^\bullet \partial \tau^\bullet} = 0 \tag{B.11}$$

From boundary conditions (B.6a) and (B.6b) as well as Eq. (B.8) it is apparent that

$$\lambda(X^\bullet, \tau^\bullet = 0) = \exp(\eta_{\text{eff}}\chi_R \cdot X^\bullet),$$
$$\lambda(X^\bullet = 0, \tau^\bullet) = \exp(\eta_{\text{eff}}\chi_R\chi_D \cdot \tau^\bullet) \tag{B.12}$$

Equation (B.11) may be solved with boundary conditions (B.12) to yield (Grubecki, 2020):

$$\lambda(X^\bullet, \tau^\bullet) = \exp(\eta_{\text{eff}}\chi_R \cdot X^\bullet) + \exp(\eta_{\text{eff}}\chi_R\chi_D \cdot \tau^\bullet) - 1 \tag{B.13}$$

Using Eq. (B.10) and returning to the untransformed variables, we obtain expressions for the hydrogen peroxide and enzyme concentrations:

$$S(X, \tau) = \frac{\exp[\eta_{\text{eff}}\chi_R\chi_D \cdot (\tau - X)]}{\exp(\eta_{\text{eff}}\chi_R \cdot X) + \exp[\eta_{\text{eff}}\chi_R\chi_D \cdot (\tau - X)] - 1} \tag{B.14}$$

$$E(X, \tau) = \frac{\exp(\eta_{\text{eff}}\chi_R \cdot X)}{\exp(\eta_{\text{eff}}\chi_R \cdot X) + \exp[\eta_{\text{eff}}\chi_R\chi_D \cdot (\tau - X)] - 1} \tag{B.15}$$

REFERENCES

Agrawal K., Verma P., 2019. Column bioreactor of immobilized *Stropharia* sp. ITCC 8422 on natural biomass support of *L. cylindrica* for biodegradation of anthraquinone violet R. *Bioresour. Technol. Rep.*, 8, 1003450. DOI: 10.1016/j.biteb.2019.100345.

Arvin E., Lars-Flemming P., 2015. Hydrogen peroxide decomposition kinetics in aquaculture water. *Aquacult. Eng.*, 64, 1–7. DOI: 10.1016/j.aquaeng.2014.12.004.

Baral B., Nial P.S., Subudhi U., 2023. Enhanced enzymatic activity and conformational stability of catalase in presence of tetrahedral DNA nanostructures: A biophysical and kinetic study. *Int. J. Biol. Macromol.*, 242, 124677. DOI: 10.1016/j.ijbiomac.2023.124677.

Carrazco-Escalante M., Caro-Corrales J., Iribe-Salazar R., Ríos-Iribe E., Vázquez-López Y., Gutiérrez-Dorado R., Hernández-Calderón O., 2019. A new approach for describing and solving the reversible Briggs-Haldane mechanism using immobilized enzyme. *Can. J. Chem. Eng.*, 98, 316–329. DOI: 10.1002/cjce.23528.

Carrié M., Velly H., Ben-Chaabane F., Gabelle J.-C., 2022. Modeling fixed bed bioreactors for isopropanol and butanol production using Clostridium beijerinckii DSM 6423 immobilized on polyurethane foams. *Biochem. Eng. J.*, 180, 108355. DOI: 10.1016/j.bej.2022.108355.

Coutu A., Dochain D., Mottelet S., André L., Mercier-Huat M., Pauss A., Ribeiro T., 2023. Dynamical model development and parameter identification for solid-state anaerobic digestion of shellfish products: Application to *Mytilus edulis*. *Bioresour. Technol. Rep.*, 22, 101458. DOI: 10.1016/j.biteb.2023.101458.

Danial E.N., Alkhalaf M.I., 2020. Co-immobilisation of superoxide dismutase and catalase using an in vitro encapsulation protocol. *J. King Saud Univ. Sci.*, 32, 2489–2494. DOI: 10.1016/j.jksus.2020.04.003.

De Prá M.C., Bonassa G., Bortoli M., Soares H.M., Kunz A., 2021. Novel one-stage reactor configuration for deammonification process: Hydrodynamic evaluation and fast start-up of NITRAMMOX®reactor. *Biochem. Eng. J.*, 171, 108005. DOI: 10.1016/j.bej.2021.108005.

Do D.D., Weiland R.H., 1981a. Catalyst deactivation in an isothermal CSTR with first-order chemical kinetics. *Chem. Eng. J.*, 21, 115–122. DOI: 10.1016/0300-9467(81)80042-1.

Do D.D., Weiland R.H., 1981b. Fixed bed reactors with catalyst poisoning: First order kinetics. *Chem. Eng. Sci.*, 36, 97–104. DOI: 10.1016/0009-2509(81)80051-6.

Eberhardt A.M., Pedroni V., Volpe M., Ferreira M.L., 2004. Immobilization of catalase from *Aspergillus niger* on inorganic and biopolymeric supports for H_2O_2 decomposition. *Appl. Catal., B*, 47, 153–163. DOI: 10.1016/j.apcatb.2003.08.007.

Fruhwirth G., Paar A., Gudelj M., Cavaco-Paulo A., Robra K.-H., Gübitz G., 2002. An immobilized catalase peroxidase from the alkalothermophilic *Bacillus* SF for the treatment of textile-bleaching effluents. *Appl. Microbiol. Biotechnol.*, 60, 313–319. DOI: 10.1007/s00253-002-1127-0.

George P., 1947. Reaction between catalase and hydrogen peroxide. *Nature*, 160, 41–43. DOI: 10.1038/160041a0.

Ghadermarzi M., Moosavi-Movahedi A.A., 1996. Determination of the kinetic parameters for the "suicide substrate" inactivation of bovine liver catalase by hydrogen peroxide. *J. Enzym Inhib.*, 10, 167–175. DOI: 10.3109/14756369609030310.

Goldsmith M., Tawfik D.S., 2017. Enzyme engineering: reaching the maximal catalytic efficiency peak. *Curr. Opin. Struct. Biol.*, 47, 140–150. DOI: 10.1016/j.sbi.2017.09.002.

Grigoras A.G., 2017. Catalase immobilization – A review. *Biochem. Eng. J.*, 117, 1–20. DOI: 10.1016/j.bej.2016.10.021.

Grubecki I., 2010a. Comparison between isothermal and optimal temperature policy for batch process with parallel (bio)-catalyst deactivation. *J. Chem. Eng. Jpn.*, 43, 1014–1019. DOI: 10.1252/jcej.08we219.

Grubecki I., 2010b. Optimal temperature control in a batch bioreactor with parallel deactivation of enzyme. *J. Process Control*, 20, 573–584. DOI: 10.1016/j.jprocont.2010.02.009.

Grubecki I., 2016. How to run biotransformations – At the optimal temperature control or isothermally? Mathematical assessment. *J. Process Control*, 44, 79–91. DOI: 10.1016/j.jprocont.2016.05.005.

Grubecki I., 2017. External mass transfer model for hydrogen peroxide decomposition by Terminox Ultra catalase in a packed-bed reactor. *Chem. Process Eng.*, 38, 307–319. DOI: 10.1515/cpe-2017-0024.

Grubecki I., 2018a. Optimal feed temperature for an immobilized enzyme fixed-bed reactor: A case study on hydrogen peroxide decomposition by commercial catalase. *Chem. Process Eng.*, 39, 39–57. DOI: 10.24425/119098.

Grubecki I., 2018b. Optimal feed temperature for hydrogen peroxide decomposition process occurring in the bioreactor with fixed-bed of commercial catalase: A case study on thermal deactivation of enzyme. *Chem. Process Eng.*, 39, 491–501. DOI: 10.24425/cpe.2018.124974.

Grubecki I., 2020. Analytical determination of the optimal feed temperature for hydrogen peroxide decomposition process occurring in bioreactor with a fixed-bed of commercial catalase. *Catalysts*, 11, 35. DOI: 10.3390/catal11010035.

Grubecki I., Wójcik M., 2013. How much of enzyme can be saved in the process with the optimal temperature control? *J. Food Eng.*, 116, 255–259. DOI: 10.1016/j.jfoodeng.2012.12.019.

Harmand J., Dochain D., 2005. The optimal design of two interconnected (bio)chemical reactors revisited. *Comput. Chem. Eng.*, 30, 70–82. DOI: 10.1016/j.compchemeng.2005.08.003.

Harmand J., Rapaport A., Dochain D., Lobry C., 2008. Microbial ecology and bioprocess control: Opportunities and challenges. *J. Process Control*, 18, 865–875. DOI: 10.1016/j.jprocont.2008.06.017.

Illanes A., Wilson L., Vera C., 2014. *Problem solving in enzyme biocatalysis*. 1st edition, John Wiley & Sons Ltd, Chichester, United Kingdom. DOI: 10.1002/9781118341742.

Leipold J., Seidel C., Nikolic D., Seidel-Morgenstern A., Kienle A., 2023. Optimization of methanol synthesis under forced periodic operation in isothermal fixed-bed reactors. *Comput. Chem. Eng.*, 175, 108285. DOI: 10.1016/j.compchemeng.2023.108285.

Li M., Christofides P.D., 2008. Optimal control of diffusion-convection-reaction processes using reduced-order models. *Comput. Chem. Eng.*, 32, 2123–2135. DOI: 10.1016/j.compchemeng.2007.10.018.

Lima P.S., Inacio A.T., Moreira Y.C., César D.E., Dias R.J.P., Dezotti M., Bassin J.P., 2021. Upgrade of a suspended biomass reactor with limited nitrification to a biofilm system: Addressing critical parameters and performance in different reactor configurations. *Biochem. Eng. J.*, 170, 107987. DOI: 10.1016/j.bej.2021.107987.

Liu C., Tian H., Gu X., Li N., Zhao X., Lei M., Alharbi H., Megharaj M., He W., Kuzyakov Y., 2022. Catalytic efficiency of soil enzymes explains temperature sensitivity: Insights from physiological theory. *Sci. Total Environ.*, 822, 153365. DOI: 10.1016/j.scitotenv.2022.153365.

Malikkides C.O., Weiland R.H., 1982. On the mechanism of immobilized glucose oxidase deactivation by hydrogen peroxide. *Biotechnol. Bioeng.*, 24, 2419–2439. DOI: 10.1002/bit.260241109.

Maria G., Crisan M., 2015. Evaluation of optimal operation alternatives of reactors used for D-glucose oxidation in a bienzymatic system with a complex deactivation kinetics. *Asia-Pac. J. Chem. Eng.*, 10, 22–44. DOI: 10.1002/apj.1825.

Mazziero V.T., Batista V.G., de Oliveira D.G., Scontri M., de Paula A.V., Cerri M.O., 2022. Characterization of packed-bed in the downcomer of a concentric internal-loop airlift bioreactor. *Biochem. Eng. J.*, 181, 108407. DOI: 10.1016/j.bej.2022.108407.

Mehrotra R., Richezzi M., Palopoli C., Hureau C., Signorella S.R., 2020. Effect of coordination dissymmetry on the catalytic activity of manganese catalase mimics. *J. Inorg. Biochem.*, 213, 111264. DOI: 10.1016/j.jinorgbio.2020.111264.

Miłek J., 2018. Estimation of the kinetic parameters for H_2O_2 enzymatic decomposition and for catalase deactivation. *Braz. J. Chem. Eng.*, 35, 995–1004. DOI: 10.1590/0104-6632.20180353s20160617.

Miłek J., 2020. Thermal deactivation of *Saccharomyces cerevisiae* catalase. *Przem. Chem.*, 99, 128–130. DOI: 10.15199/62.2020.3.17.

Ordaz A., Ramirez R., Hernandez-Martinez G.R., Carrión M., Thalasso F., 2019. Characterization of kinetic parameters and mass transfer resistance in an aerobic fixed-bed reactor by *in-situ* respirometry. *Biochem. Eng. J.*, 146, 194–202. DOI: 10.1016/j.bej.2019.03.024.

Ortega R., Bobtsov A., Nikolaev N., Schiffer J., Dochain D., 2021. Generalized parameter estimation-based observers: Application to power systems and chemical–biological reactors. *Automatica*, 129, 109635. DOI: 10.1016/j.automatica.2021.109635.

Razavi B.S., Blagodatskaya E., Kuzyakov Y., 2016. Temperature selects for static soil enzyme systems to maintain high catalytic efficiency. *Soil Biol. Biochem.*, 97, 15–22. DOI: 10.1016/j.soilbio.2016.02.018.

Robles A., Capson-Tojo G., Ruano M.V., Latrille E., Steyer J.P., 2018. Development and pilot-scale validation of a fuzzy-logic control system for optimization of methane production in fixed-bed reactors. *J. Process Control*, 68, 96–104. DOI: 10.1016/j.jprocont.2018.05.007.

Samson M., Yang T., Omar M., Xu M., Zhang X., Alphonse U., Rao Z., 2018. Improved thermostability and catalytic efficiency of overexpressed catalase from *B. pumilus* ML 413 (KatX2) by introducing disulfide bond C286-C289. *Enzyme Microb. Technol.*, 119, 10–16. DOI: 10.1016/j.enzmictec.2018.08.002.

Schorsch J., Castro C.C., Couto L.D., Nobre C., Kinnaert M., 2019. Optimal control for fermentative production of fructo-oligosaccharides in fed-batch bioreactor. *J. Process Control*, 78, 124–138. DOI: 10.1016/j.jprocont.2019.03.004.

Sooch B.S., Kauldhar B.S., Puri M., 2014. Recent insights into microbial catalases: Isolation, production and purification. *Biotechnol. Adv.*, 32, 1429–1447. DOI: 10.1016/j.biotechadv.2014.09.003.

Sun B., Zhu H., Jin Y., Qiao K., Xu W., Jiang J., 2019. Rapid hydrogen peroxide decomposition using a microreactor. *Chem. Eng. Technol.*, 42, 252–256. DOI: 10.1002/ceat.201800319.

Tezer Ö., Karabağ N., Öngen A., Ayol A., 2023. Gasification performance of olive pomace in updraft and downdraft fixed bed reactors. *Int. J. Hydrogen Energy*, 48, 22909-22920. DOI: 10.1016/j.ijhydene.2023.02.088.

Trawczyńska I., 2020. New method of determining kinetic parameters for decomposition of hydrogen peroxide by catalase. *Catalysts*, 10, 323. DOI: 10.3390/catal10030323.

Vasudevan P.T., Weiland R.H., 1990. Deactivation of catalase by hydrogen peroxide. *Biotechnol. Bioeng.*, 36, 783–789. DOI: 10.1002/bit.260360805.

Vishnu Priya B., Sreenivasa Rao D.H., Gilani R., Lata S., Rai N., Akif M., Kumar Padhi S., 2022. Enzyme engineering improves catalytic efficiency and enantioselectivity of hydroxynitrile lyase for promiscuous retro-nitroaldolase activity. *Bioorg. Chem.*, 120, 105594. DOI: 10.1016/j.bioorg.2021.105594.

Xiu G.-H., Jiang L., Li P., 2001. Mass-transfer limitations for immobilized enzyme-catalyzed kinetic resolution of racemate in a fixed-bed reactor. *Biotechnol. Bioeng.*, 74, 29–39. DOI: 10.1002/bit.1092.